COMPARATIVE MINERALOGY, MICROSTRUCTURE AND COMPOSITIONAL TRENDS IN THE SUB-MICRON SIZE FRACTIONS OF MARE AND HIGHLAND LUNAR SOILS. M. S. Thompson[1], R. Christoffersen[2,4], S. K. Noble[3] and L. P. Keller[4], [1]Lunar and Planetary Laboratory, University of Arizona, 1629 E. University Blvd., Tucson AZ 85721, mst@lpl.arizona.edu, [2]Mail Code JE23, ESCG / Jacobs Technology, Houston, TX 77258-8447, [3]NASA GSFC Mail Code 691, Greenbelt MD 20771, [4]NASA JSC Mail Code KR, Houston TX 77058.

Introduction: The morphology, mineralogy, chemical composition and optical properties of lunar soils show distinct correlations as a function of grain size and origin [1,2,3]. In the <20 µm size fraction, there is an increased correlation between lunar surface properties observed through remote sensing techniques and those attributed to space weathering phenomenae [1,2]. Despite the establishment of recognizable trends in lunar grains <20 in size [1,2,3], the size fraction < 10 µm is characterized as a collective population of grains without subdivision. This investigation focuses specifically on grains in the <1 µm diameter size fraction for both highland and mare derived soils. The properties of these materials provide the focus for many aspects of lunar research including the nature of space weathering on surface properties, electrostatic grain transport [4,5] and dusty plasmas [5]. In this study, we have used analytical transmission and scanning transmission electron microscopy (S/TEM) to characterize the mineralogy type, microstructure and major element compositions of grains in this important size range in lunar soils.

Samples and Methods: The lunar soil samples selected for this study were initially dry sieved to obtain a <20 µm fraction. Sample 10084 is a representative mature mare soil (Is/FeO = 78) [3] and sample 62231 is a very mature highland soil (Is/FeO = 91) [6]. For both soil samples, settling experiments were performed in ultraclean vials of ethanol to concentrate grains <1 µm in size for TEM study. Using Stokes Law approximations, approximately 30 mg of each sample was subjected to two ours of gravity induced settling, after which a droplet was withdrawn with a glass pipette and placed on a continuous carbon film TEM grid. The ethanol suspension was then evaporated over several hours. TEM observations confirmed that this method produced a high concentration of <1 µm grains that were sufficiently thin for quantitative energy dispersive x-ray analyses (EDX). Grains below a threshold of 1.0 µm in diameter were randomly selected and subjected to digital bright-field imaging and EDX analysis. Peak intensities were converted to element concentrations using the Cliff-Lorimer method [7]. The 10084 analyses were obtained using a JEOL 2000FX TEM, while the 62231 sample analyses were collected on the JEOL 2500 STEM, both instruments are equipped with Noran thin-window EDX detectors.

Chemical Composition and Type of Sub-Micrometer Grains: A total of 400 grains were analyzed: 200 for each of the 10084 and 62231 samples. Grains were individually imaged and chemically analyzed. Both samples' overall modal composition is compared to data for larger size fractions (Figure 1).

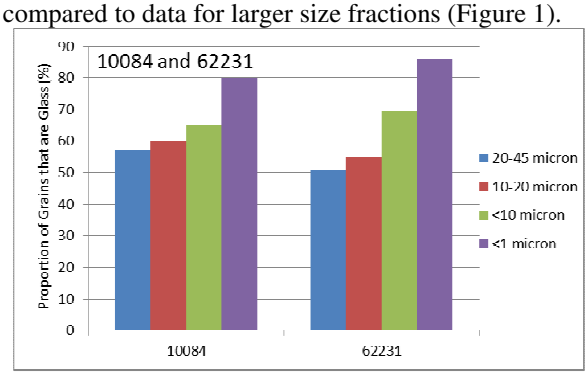

Figure 1: *Modal composition of <1 µm grains in lunar soil samples 10084 and 62231 as compared to larger size fractions.*

Soil 10084: A total of 80% of analyzed grains are classified as glass which constitutes a significant increase in this grain type from 65% in the <10 µm size fraction [3]. The remaining grains are mineral fragments, predominantly plagioclase, with lesser amounts of ilmenite, pyroxene and olivine. The large proportion of glass grains in this size fraction lead our team to focus our investigation on the chemical and morphological properties of this material. On a morphological basis, 45% of these glass grains (36% of total population) belong to a subpopulation of spherules that exhibit limited evidence of nanophase Fe metal (Fe^0) (Figure 2). The majority of remaining material is irregularly shaped grains that contain varying amounts of nanophase Fe^0 (Figure 3). A small component of the glass population (<10%) are hybrid types (i.e spherules with nanophase Fe^0).

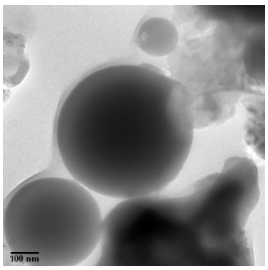

Figure 2*: Bright field TEM images of <1 um glass spherules in lunar soil 10084.*

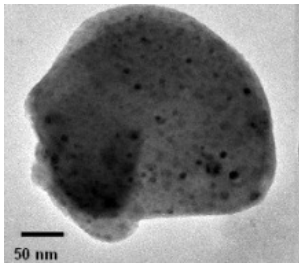

Figure 3: *Bright-field TEM images of glass grain containing nanophase Fe^0.*

Soil 62231: A total of 85% of analyzed grains are classified as types of glass, constituting an increase in this material from the 70% in the <10 µm size fraction (Figure 1) [6]. The remaining material is composed of mineral fragments. Morphologically, ~20% of glass grains (17% of total) are spherical in shape and exhibit very little nanophase Fe^0. The majority of remaining glass is irregularly shaped and contains prominent nanophase Fe^0. A small component of the glass population(<15%) represents hybrid types (Figure 4). In addition, a small proportion of glass grains (<3%) exhibited vesiculated morphologies (Figure 5).

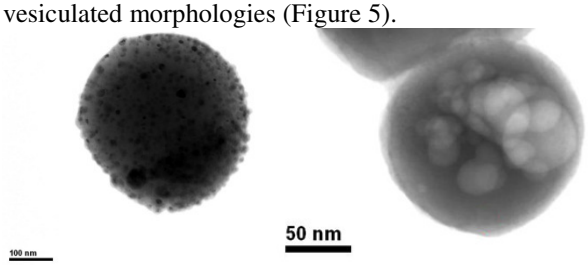

Figure 4: *Bright field TEM image of a hybrid type grain in lunar sample 62231.*

Figure 5: *Bright field TEM image of a vesiculated glass grain in lunar sample 62231.*

Composition and Chemical Variation Trends of Glass Grains: The predominance of homogeneous glass grains allowed us to use EDX analyses to compositionally characterize the particles based on previous studies of sub-µm lunar glass grains [8,9]. Previous work has identified two major compositional classes of lunar glass grains. One group is associated with impact melting, generating a glass grain that primarily retains the elemental composition of the parent material in the new grain. Material in the second group is considered to form from volatilization and vapor condensation processes which generate a significant and predictable chemical evolution with respect to volatile content. A higher Al_2O_3 and CaO content is indicative of volatile loss seen in the HASP glasses (High Aluminum Silica Poor). In contrast to HASP, high FeO and SiO_2 content is considered to indicate VRAP (Volatile-Rich-Al-Poor) and Pseudo-VRAP grains [8,9]. Plotting compositions based on these chemical parameters allows us to identify glasses with HASP and VRAP affinities at the upper and lower ends of the data trend respectively (Sample 10084 - Figure 6, Sample 62231- Figure 7). The data collected identifies approximately 28% HASP grains and 12% VRAP grains in the total glass grain population of sample 10084. The significant proportion of these volatile-affected grains supports the idea that high surface area-to-volume ratio is necessary to promote these vapor-mediated chemical changes. Despite a similar maturity level, sample 62231 exhibits a significantly smaller proportion of material affected by volatilization mechanisms, with 9% HASP grains and 10% VRAP grains. This suggests volatilization may be dependant on initial rock composition and/or may not be uniform across the lunar surface. The HASP grains can be further subdivided into highland or mare affinity based on total $FeO+MgO+TiO_2$ content and CaO/Al_2O_3 ratio. A significant proportion (20%) of the HASP glasses in 10084 mare sample display a highland-affinity, indicating significant mixing at this small size fraction [2]. In support of this, a high proportion (26%) of the HASP glasses in the 62231 highland sample display a mare-affinity. The remaining glassy material is of compositional type in the middle of the trend, and is unaffected by volatilization. A sub-population in this group falls off the trend line and may be "monomineralic" melts from single mineral grains.

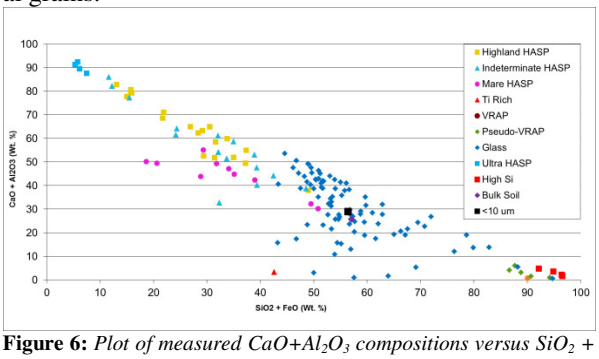

Figure 6: *Plot of measured $CaO+Al_2O_3$ compositions versus SiO_2 + FeO for all sub-micron 10084 soil glass grains.*

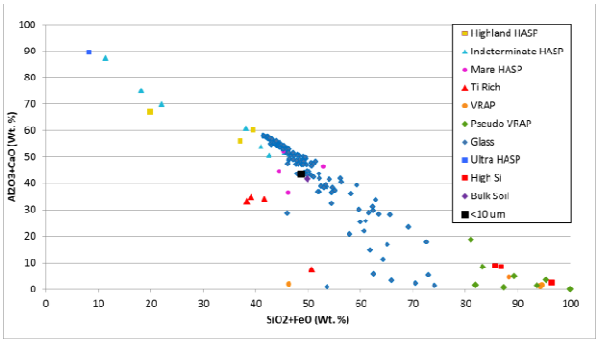

Figure 7: *Plot of measured $CaO+Al_2O_3$ compositions versus SiO_2 + FeO for all sub-micron 62231 soil glass grains.*

References: [1] Taylor, L.A et al. (2001) Met. & Planet. Sci., v. 36, 285-299. [2] Pieters C. M. and Taylor L. A. (2003) GRL 30:20, 2048, [3] Taylor L.A. et al (2001) JGR, 106, 27985-28000. [4] Stubbs T. J. et al. (2006) Adv. Space Research, 37, 59-66. [5] Horanyi M. (1996) Ann. Rev. Astrn. and Aphys., 34, 383-418. [6] Taylor, L.A et al. (2010) JGR, 115. [7] Cliff, G. and Lorimer, G.W. (1975) J. Microscopy, v. 103, 203. [8] Norris J.A., Keller L.P. and McKay D.S (1992) Lunar Science Inst. Workshop on the Geology of the Apollo 17 Landing Site, p. 44-45 [9] Norris J.A., Keller L.P. And McKay D.S (1993). Lunar and Planetary Institute- 24th LPSC, Part 3, p. 1093-1094.